Inorg. Chem. **2008**, *47*, 2155−2161

Interaction of Dichloride Iron(II) Clathrochelate with Dimercaptomaleodinitrile: Synthesis of the Precursor Monoribbed-Functionalized Phthalocyaninoclathrochelates and the Unexpected Formation of a New Thiophene-Containing Heterocyclic System in the Ribbed Chelate Fragment of the Clathrochelate Framework

Yan Z. Voloshin,*,† Oleg A. Varzatskii,‡ Alexander S. Belov,† Zoya A. Starikova,† Kyrill Y. Suponitsky,† Valentin V. Novikov,† and Yurii N. Bubnov†

Nesmeyanov Institute of Organoelement Compounds, 119991, Moscow, Russia, and Vernadskii Institute of General and Inorganic Chemistry, Kiev-142, 03680, Ukraine

Received July 22, 2007

Clathrochelate iron(II) $FeBd_2(S_2C_2(CN)_2Gm)(BF)_2$ tris-dioximate with a ribbed *vic*-dinitrile fragment was synthesized as a precursor of the monoribbed-functionalized hybrid phthalocyaninoclathrochelates by nucleophilic substitution of the *vic*-dichloride $FeBd_2(Cl_2Gm)(BF)_2$ clathrochelate (**1**) with the potassium salt of dimercaptomaleodinitrile. Reaction of nitromethane with this salt was followed by the condensation of the reaction products with **1** to yield the clathrochelate with an annulated previously unknown thiazinothiophene heterocyclic system in the ribbed fragment. Both complexes were characterized on the basis of elemental analysis; MALDI-TOF mass spectrometry; IR, UV–vis, ^{57}Fe Mössbauer, and NMR spectroscopies; and X-ray crystallography.

Introduction

Molecular electronics aims at designing molecular structures exhibiting a variety of physical characteristics. This allows for the creation of devices that convert electron and energy transfer processes into a logic function of electrical signals. Controlling the direction of the current or the localization of the charges in a molecular assembly in response to one or several input signals results in the development of a new concept of logic gates at the molecular level. The characteristics of polynuclear metal complexes determine their great potential in molecular logic devices: metal ion centers are sensitive to photoexcitation as well as to changes in the pH and electrochemical potential.[1−10] In the case of polyenic clathrochelate complexes (i.e., three-dimensional complexes with the encapsulated metal ion coordinating five or more nitrogen and/or sulfur donor atoms of not less than three macrocyclic fragments of an encapsulating ligand[11]), the rigid macrobicyclic framework of metal tris-dioximates, tris-oximehydrazonates, and tris-azineoximates allows one to fine-tune the spatial positions of the substituents at this framework, the parts, and the fragments of clathrochelate molecules. These features make such systems especially attractive for the design of highly integrated molecular logic gates.

Logic cells of this type can be constructed on the basis of polynuclear clathrochelates, which are the derivatives of ribbed-functionalized clathrochelates. The substituents in

* To whom correspondence should be addressed. E-mail: voloshin@ineos.ac.ru.
† Nesmeyanov Institute.
‡ Vernadskii Institute.

(1) Low, P. J. *Dalton Trans.* **2005**, 2821.
(2) Braun-Sand, S. B.; Wiest, O. *J. Phys. Chem. B* **2003**, *107*, 9624.
(3) Lau, V. C.; Berben, L. A.; Long, J. R. *J. Am. Chem. Soc.* **2003**, *124*, 9042.
(4) Raymo, F. M. *Adv. Mater.* **2002**, *14*, 401.
(5) Balzani, V.; Credi, A.; Venturi, M. *Chem. Phys. Chem.* **2003**, *4*, 49.
(6) de Silv, A. P.; McClenaghan, N. D. *Chem.—Eur. J.* **2004**, *10*, 574.
(7) de Silva, A. P. *Nat. Mater.* **2005**, *4*, 15.
(8) Ellenbogan, J. C.; Love, J. C. *Proc. IEEE* **2000**, *88*, 386.
(9) Lent, C. S.; Isaksen, B.; Lieberman, M. *J. Am. Chem. Soc.* **2003**, *125*, 1056.
(10) Jiao, J.; Long, G. J.; Rebbouh, L.; Grandjean, F.; Beatty, A. M.; Fehlner, T. P. *J. Am. Chem. Soc.* **2005**, *127*, 17819.
(11) Voloshin, Y. Z.; Kostromina, N. A.; Krämer, R. *Clathrochelates: Synthesis, Structure, and Properties*; Elsevier: Amsterdam, 2002.

10.1021/ic701452g CCC: $40.75
Published on Web 01/17/2008

Table 1. Crystallographic Data and Experimental Details for Clathrochelates **2** and **3**

	2	**3**
empirical formula	$C_{34}H_{20}B_2F_2FeN_8O_6S_2 \cdot 2.5C_6H_6$	$C_{35}H_{21}B_2F_2FeN_9O_8S_2 \cdot 2.5C_3H_6O \cdot 0.5n\text{-}C_7H_{16}$
fw	1011.44	1070.49
temp (K)	120	100
color, habit	dark orange, plate	dark red, plate
cryst dimens (mm^3)	0.25 × 0.20 × 0.05	0.20 × 0.15 × 0.05
cryst syst	triclinic	triclinic
space group	$P\bar{1}$	$P\bar{1}$
a (Å)	11.876(2)	11.931(1)
b (Å)	16.576(3)	11.972(1)
c (Å)	26.185(5)	19.233(2)
α (deg)	89.197(6)	80.312(2)
β (deg)	76.916(5)	80.917(2)
γ (deg)	69.042(4)	68.869(2)
V ($Å^3$)	4676(2)	2511.7(4)
Z	4	2
D_{cal} (g cm^{-3})	1.437	1.415
$F(000)$	2076	1106
μ (mm^{-1})	4.80	4.57
min/max transmn coeff	0.813/0.976	0.892/0.977
$2\theta_{max}$ (deg)	52.00	54.00
reflns collected	28 224	25 811
indep reflns (R_{int})	18 049 (0.0716)	10 785 (0.0722)
refined params	1105	690
R_1[a] [$I > 2\sigma(I)$]	0.0712 (5827 reflns)	0.0689 (6598 reflns)
R_w[b] (all data)	0.0996	0.1575
GOF[c]	0.961	1.038
max/min residual peak	0.459 and –0.383	1.325 and –0.629

[a] $R_1 = (\sum||F_o| - |F_c||)/\sum|F_o|$. [b] $R_w = [\sum(w(F_o^2 - F_c^2)^2)/\sum w(F_o^2)^2]^{1/2}$. [c] GOF $= [\sum(w(F_o^2 - F_c^2)^2)/(N_{obsd} - N_{param})]^{1/2}$.

chelate (ribbed) fragments of polyenic clathrochelates have substantial steric and electronic effects on the polyhedron geometry and central metal ion properties due to the direct interaction of the highly conjugated π-system of a ligand and the π- and σ-systems of the ribbed substituents. One has an opportunity to use such substituents to change the encapsulated metal ion properties and to affect the electronic (and, therefore, the donor) characteristics of these substituents by changing an encapsulated metal ion electronic configuration via redox transitions.[12] Varying the ribbed substituents at a clathrochelate framework has been recognized as a unique opportunity to stabilize unusual oxidation states of an encapsulated metal ion. In particular, a new approach to the synthesis of air-stable cobalt(I) complexes used a macrobicyclic hexachloride ligand with six strongly electron-withdrawing substituents in chelate π-conjugated α-dioximate fragments.[13] Di- and triribbed-functionalized macrobicyclic iron and ruthenium(II) mono-, di-, tri-, tetra-, and hexa-substituted tris-dioximates have previously been obtained starting from their reactive tri- and hexachloride clathrochelate precursors.[12,14–20] Monoribbed-functionalized (i.e., containing one or two functionalizing substituents in one of the three dioximate fragments) iron(II) clathrochelates have also been synthesized starting from the corresponding mono- and dichloride precursors.[18–23] The synthesis of ribbed-functionalized clathrochelates with substituents, which are able to coordinate a metal ion to produce polynuclear complexes with interaction through the clathrochelate framework metal centers, is of particular interest.[12] We have attempted to obtain a series of macrobicyclic monoribbed-functionalized iron(II) tris-dioximates with a ribbed *vic*-dinitrile fragment, in particular, in the present study, to synthesize complex **2**, as a precursor of the monoribbed-functionalized hybrid phthalocyaninoclathrochelates, under different reaction conditions. Moreover, it was an unexpected success that we isolated a chlathrochelate with an annulated heterocyclic system of a new type when we changed the reaction conditions. Such types of substituents are very important for the design of DNA intercalators as well.

Experimental Procedures

General Procedures. The reagents used, $FeCl_2 \cdot 4H_2O$, α-benzyldioxime (H_2Bd), $BF_3 \cdot O(C_2H_5)_2$, sorbents, and organic solvents, were obtained commercially (Fluka). The dichloroglyoxime (de-

(12) Voloshin, Y. Z.; Varzatskii, O. A.; Kron, T. E.; Belsky, V. K.; Zavodnik, V. E.; Palchik, A. V. *Inorg. Chem.* **2000**, *39*, 1907.
(13) Voloshin, Y. Z.; Varzatskii, O. A.; Vorontsov, I. I.; Antipin, M. Y. *Angew. Chem., Int. Ed.* **2005**, *44*, 3400.
(14) Voloshin, Y. Z.; Varzatskii, O. A.; Palchik, A. V.; Stash, A. I.; Belsky, V. K. *New J. Chem.* **1999**, *23*, 355.
(15) Voloshin, Y. Z.; Varzatskii, O. A.; Kron, T. E.; Belsky, V. K.; Zavodnik, V. E.; Strizhakova, N. G.; Nadtochenko, V. A.; Smirnov, V. A. *Dalton Trans.* **2002**, 1203.
(16) Voloshin, Y. Z.; Varzatskii, O. A.; Palchik, A. V.; Strizhakova, N. G.; Vorontsov, I. I.; Antipin, M. Y.; Kochubey, D. I.; Novgorodov, B. N. *New J. Chem.* **2003**, *27*, 1148.
(17) Voloshin, Y. Z.; Varzatskii, O. A.; Vorontsov, I. I.; Antipin, M. Y.; Lebedev, A. Y.; Belov, A. S.; Strizhakova, N. G. *Russ. Chem. Bull. Int. Ed.* **2004**, *53*, 92.
(18) Voloshin, Y. Z.; Zavodnik, V. E.; Varzatskii, O. A.; Belsky, V. K.; Vorontsov, I. I.; Antipin, M. Y. *Inorg. Chim. Acta* **2001**, *321*, 116.
(19) Voloshin, Y. Z.; Varzatskii, O. A.; Palchik, A. V.; Vorontsov, I. I.; Antipin, M. Y.; Lebed, E. G. *Inorg. Chim. Acta* **2005**, *358*, 131.
(20) Voloshin, Y. Z.; Varzatskii, O. A.; Palchik, A. V.; Starikova, Z. A.; Antipin, M. Y.; Lebed, E. G.; Bubnov, Y. N. *Inorg. Chim. Acta* **2006**, *359*, 553.
(21) Voloshin, Y. Z.; Zavodnik, V. E.; Varzatskii, O. A.; Belsky, V. K.; Palchik, A. V.; Strizhakova, N. G.; Vorontsov, I. I.; Antipin, M. Y. *Dalton Trans.* **2002**, 1193.
(22) Voloshin, Y. Z.; Belov, A. S.; Lebedev, A. Y.; Varzatskii, O. A.; Antipin, M. Y.; Starikova, Z. A.; Kron, T. E. *Russ. Chem. Bull. Int. Ed.* **2004**, *53*, 1171.
(23) Voloshin, Y. Z.; Varzatskii, O. A.; Starikova, Z. A.; Antipin, M. Y.; Lebedev, A. Y.; Belov, A. S. *Russ. Chem. Bull. Int. Ed.* **2004**, *53*, 1439.

Scheme 1

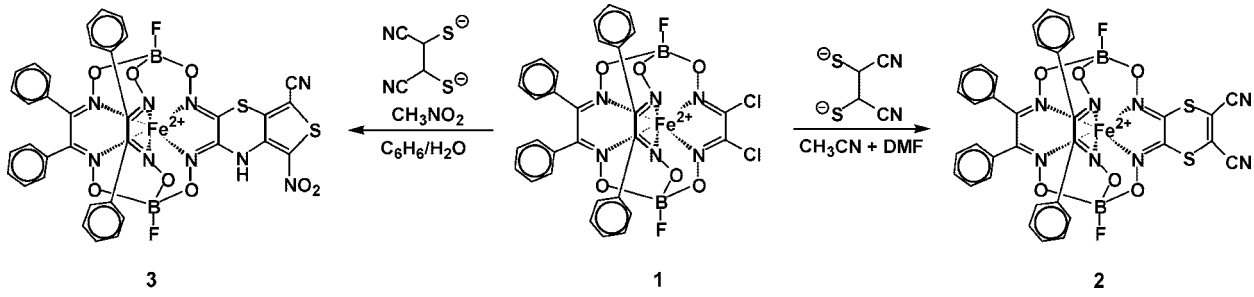

Scheme 2

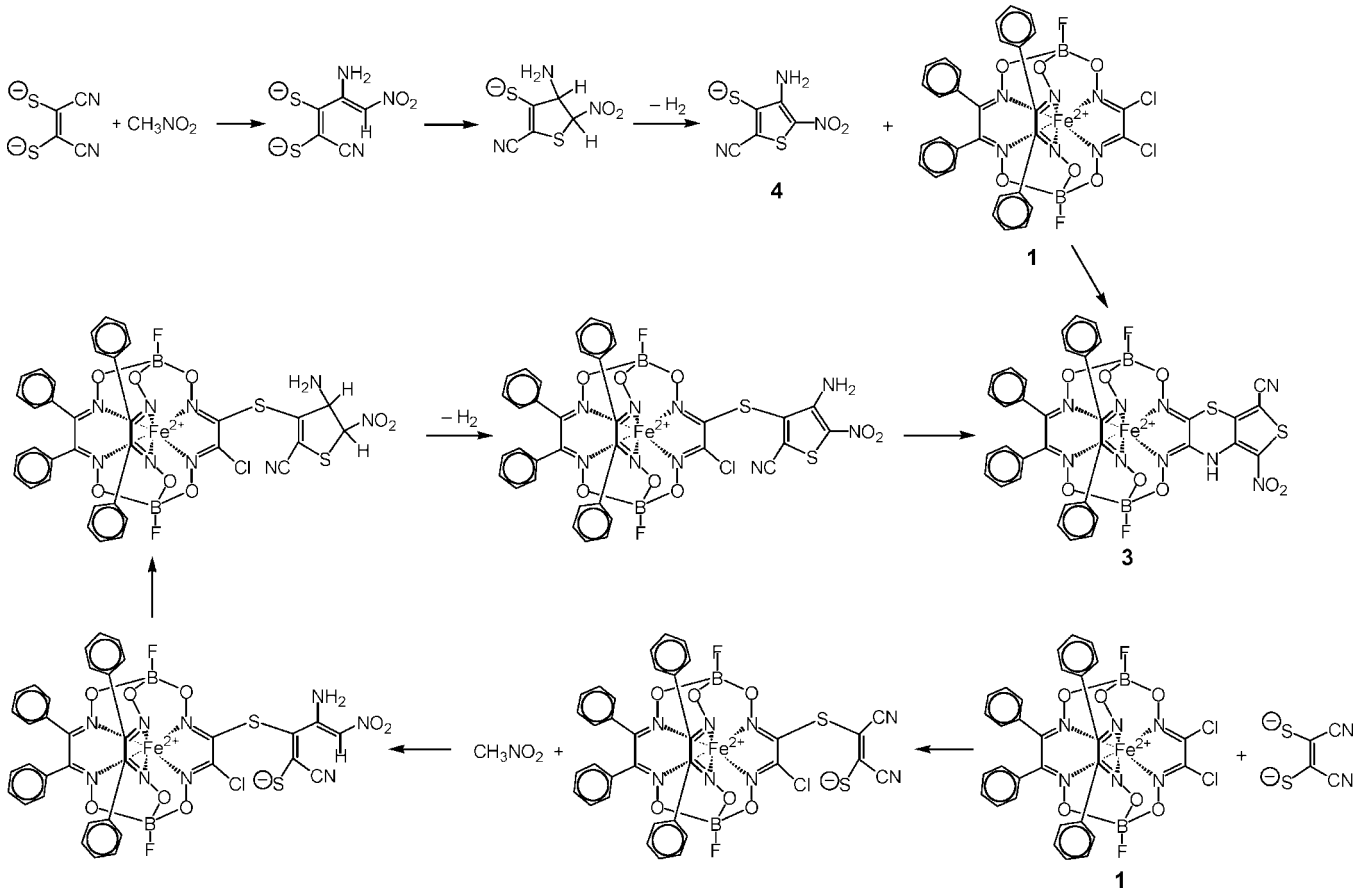

Scheme 3

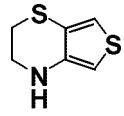

5

noted as H_2Cl_2Gm) was obtained by chlorination of glyoxime (H_2Gm) as described in ref 24. The complex $FeBd_2(Cl_2Gm)(BF)_2$ (**1**) was prepared as described in ref 21. Potassium salt of dimercaptomaleodinitrile was synthesized as described in ref 25.

Analytical data (C, H, and N contents) were obtained with a Carlo Erba model 1106 microanalyzer. The iron content was determined spectrophotometrically with 5-sulfosalicylic acid.[26,27] The MALDI-TOF, IR, UV–vis, NMR, and Mössbauer data were obtained as described previously[20] (see Supporting Information).

Syntheses. $FeBd_2(S_2C_2(CN)_2Gm)(BF)_2$ (2). The complex $FeBd_2(Cl_2Gm)(BF)_2$ (**1**) (0.75 g, 1 mmol) was dissolved/suspended in acetonitrile (25 mL), and then the solution of potassium salt of mercaptomaleodinitrile (0.26 g, 1.2 mmol) in dry DMF (10 mL) was added under argon. The reaction mixture was stirred for 40 min and then precipitated with water (50 mL). The precipitate was filtered, dried in air, and extracted with methylene dichloride (40 mL, in two portions). The extract was dried with Na_2SO_4 and rotary evaporated to dryness. The solid residue was dissolved in methylene dichloride, and the solution was filtered through Silasorb SPH-300 (eluent: methylene dichloride−hexane 7:3 mixture). The head dark-orange elute was rotary evaporated to dryness, and the solid residue was reprecipitated from methylene dichloride with hexane. The precipitate was washed with hexane and dried in vacuo. Yield:

(24) Ponzio, G.; Baldrocco, F. *Gazz. Chim. Ital.* **1930**, *60*, 415.
(25) Engler, E. M.; Patel, V. V. *Chem. Commun.* **1975**, 387.
(26) Rodionova, T. V.; Beklemishev, M. K.; Dracheva, L. V.; Zolotov, Y. A. *Zh. Anal. Khim.* **1992**, *47*, 1211.
(27) Stryjewska, E.; Krasnodebska, B.; Biala, H.; Teperek, J.; Rubel, S. *Chem. Anal.* **1994**, *39*, 483.

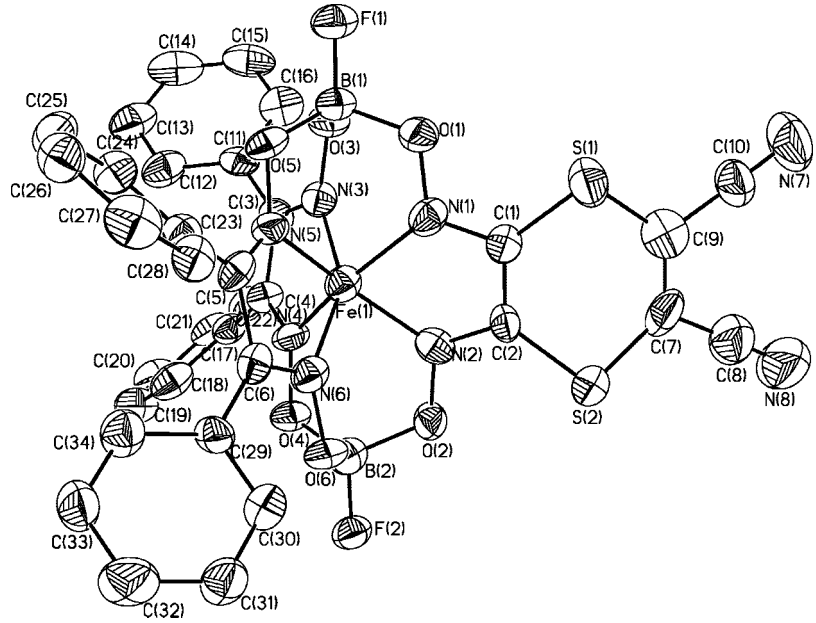

Figure 1. ORTEP view (50% probability of thermal ellipsoids) of clathrochelate molecule **2** (type A).

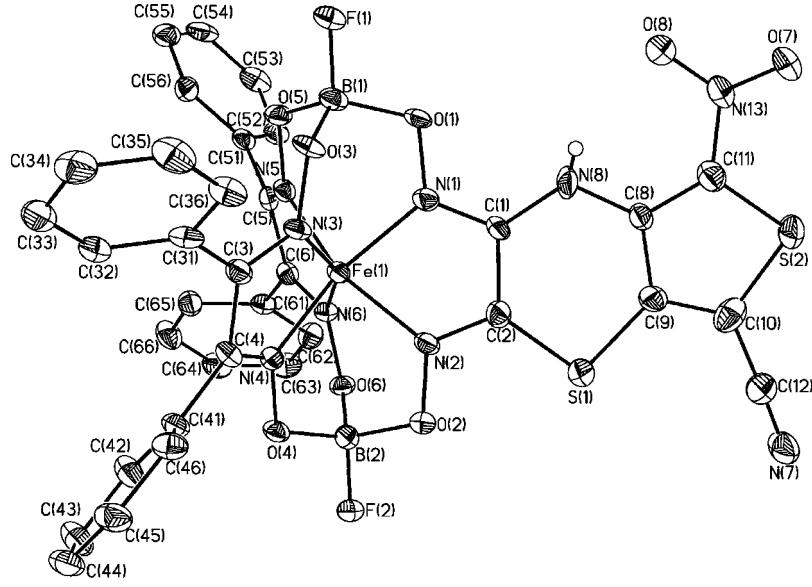

Figure 2. ORTEP view (50% probability of thermal ellipsoids) of clathrochelate molecule **3**.

0.12 g (15%). Found: C, 50.11; H, 2.48; N, 13.53; Fe, 6.80. Calcd for $C_{34}H_{20}N_8O_6S_2B_2F_2Fe$: C, 50.03; H, 2.47; N, 13.73; Fe, 6.84%. MS (MALDI-TOF): *m*/*z* (I, %): (positive range): 816(100) $[M]^{+\bullet}$; 790(30) $[M - CN]^{+\bullet}$; and 778(90) $[M - CCN]^{+\bullet}$ and (negative range): –816 $[M]^{-\bullet}$. ^1H NMR (CD_2Cl_2): δ (ppm) 7.25 (m, 20H, Ph). $^{13}C\{^1H\}$ NMR (CD_2Cl_2): δ (ppm) 111.4 (s, C≡N), 114.2 (s, C═C), 128.4 (s, Ph), 128.9, 130.4, 130.8 (three s, Ph), 132.3 (s, SC═N), 158.3 (s, PhC═N). IR (KBr): 1549 ν(SC═N), 1581 ν(PhC═N), 906, 937, 1064, 1107 ν(N−O), 1219 m ν(B−O) + ν(B−F), 2229 ν(C≡N). UV–vis (methylene dichloride): λ_{max} (10^{-3} ϵ, mol^{-1} L cm^{-1}) 234(29), 262(11), 282(15), 309(11), 402(5.1), 468(22), 513(12) nm. Mössbauer ^{57}Fe (mm s^{-1}): IS = 0.33, QS = 0.51.

$FeBd_2(TPHGm)(BF)_2$ (3). The complex $FeBd_2(Cl_2Gm)(BF)_2$ (**1**) (0.75 g, 1 mmol) was dissolved/suspended in nitromethane (10 mL), and then the potassium salt of dimercaptomaleodinitrile (0.44 g, 2 mmol) was added under argon. The reaction mixture was stirred for 2 h, and then benzene (50 mL), water (20 mL), and a 40% aqueous solution of tetra-*n*-butylammonium sulfate (0.6 mL, 0.4 mmol) were added to the reaction mixture under stirring. The reaction mixture was left for 40 h at room temperature, and the aqueous and organic phases were separated. The additional portion of the clathrochelate products was extracted with benzene (20 mL). The combined benzene extract was dried with Na_2SO_4 and rotary evaporated to dryness. The solid residue was dissolved in methylene dichloride and filtered through the Silasorb SPH-300 (eluent: methylene dichloride). The head orange-red elute was evaporated to dryness and reprecipitated from methylene dichloride with hexane. The precipitate obtained was chromatographically separated on Silasorb SPH-300 (eluent: methylene dichloride−hexane 2:1 mixture). The head dark-orange elute, containing mainly the dichloride precursor, was thrown out, and the second red-violet elute was collected. This elute was evaporated to dryness, and the solid residue was washed with a small amount of methanol and hexane and dried in vacuo. Yield: 0.20 g (23%). Found: C, 48.11; H, 2.63; N, 14.32; S, 7.26; Fe, 6.26. Calcd for $C_{36}H_{23}N_9O_7S_2B_2F_2Fe$: C,

Scheme 4

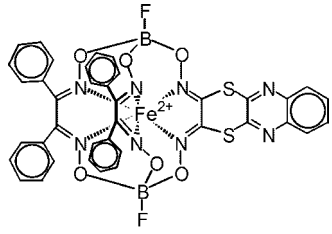

6

48.03; H, 2.42; N, 14.4; S, 7.33; Fe, 6.38%. MS (MALDI-TOF): *m/z*: (positive range) 875 $[M]^{+\bullet}$; (negative range) –874 $[M - H^+]^-$. ^1H NMR (CD_2Cl_2): δ (ppm) 10.08 (br s, 1H, NH), 7.26 (m, 20H, Ph). $^{13}C\{^1H\}$ NMR (CD_2Cl_2): δ (ppm) 106.0 (s, C≡N), 110.0 (s, *C*CN), 126.3 (s, CNO_2), 128.40, 128.41 (both s, Ph), 129.31 (s, Ph), 129.33 (s, NC*C*S), 130.0 (s, N*C*CS), 130.7 (s, Ph), 130.83, 130.86 (both s, Ph), 132.3 (s, SC═N), 135.9 (s, NC═N), 157.5 (s, PhC═N), 157.8 (s, PhC═N). IR (KBr): 1547 ν(SC═N + NC═N), 1576 ν(PhC═N), 899, 933, 1061, 1109 ν(N−O), 1221 m ν(B−O) + ν(B−F), 1620 δ(N−H), 2216 ν(C≡N). UV–vis (methylene dichloride): λ_{max} (10^{-3} ϵ, mol^{-1} L cm^{-1}) 254 (30), 283 (18), 305 (14), 335 (5.6), 365 (5.5), 392 (4.8), 440 (8.7), 479 (19), 512 (6.0), 538 (10), 571 (6.8) 601 (4.2) nm. Mössbauer ^{57}Fe (mm s^{-1}): IS = 0.36, QS = 0.63.

X-ray Crystallography. Details of the crystal data collection and refinement parameters for **2** and **3** are listed in Table 1. Single crystals of these complexes were grown from isooctane−benzene and acetone−heptane mixtures at room temperature.

The single-crystal X-ray diffraction experiments for complexes **2** and **3** were carried out with Bruker SMART 1K and SMART APEX II CCD diffractometers, using graphite monochromated Mo Kα radiation (λ = 0.710 73 Å). Reflection intensities were integrated using SAINT software[28] and corrected for absorption by semiempirical methods (SADABS program[29]).

The structures were solved by the direct method and refined by a full-matrix least-squares method against F^2 of all data, using the SHELXTL software.[30] Non-hydrogen atoms were refined with anisotropic displacement parameters. The positions of hydrogen atoms were calculated and included in refinement in isotropic approximation by the riding model with $U_{iso}(H) = nU_{eq}(C)$, where n = 1.5 for methyl groups and 1.2 for the other groups.

Results and Discussion

The easiest pathway to the precursor of the ribbed-functionalized phthalocyaninoclathrochelates is based on the condensation of reactive *vic*-clathrochelate **1** with a salt of dimercaptomaleodinitrile dianion (Scheme 1).

Despite the fact that the *vic*-dichloride iron(II) clathrochelate easily reacts with thiolate anions,[12,14–17,19–23] in CH_3CN/DMF, its nucleophilic substitution with the potassium salt of dimercaptomaleodinitrile under different conditions led to the target complex **2** only in low yield (∼15%). The formation of a mixture of byproducts with low chromatographic mobility was also observed. These side reactions are caused by nucleophilic substitutions with the trans-form of dimercaptomaleodinitrile: this results in the formation of polymeric products. Low yield was also caused by both the high reactivity and the thiophilicity of **2**; similar behavior is observed for the dichloride clathrochelate precursor **1**.

Attempts to optimize the reaction conditions by the choice of a solvent and to obtain **2** in higher yield failed. An unexpected result was obtained when nitromethane was used as a solvent: its reaction with the potassium salt of dimercaptomaleodinitrile followed by the condensation of the reaction products, which probably contain nitrothiophene **4**, with precursor **1** led to clathrochelate complex **3** with an annulated thiazinothiophene heterocycle in the ribbed fragment (Scheme 2).

The formation of clathrochelate **3** under the conditions of interphase catalysis can be explained by hindering of the dimercaptomaleodinitrile dianion−tetra-*n*-butylammonium cation ionic pair phase transfer. At the same time, the monocharged and lipophilic 2-cyano-3-mercapto-4-amino-5-nitrothiophene anion, formed by the condensation of dimercaptomaleodinitrile with nitromethane, can be efficiently transferred to the organic phase in the form of an ionic pair with the Bu_4N^+ cation followed by nucleophilic substitution with *vic*-dihalogenide clathrochelate **1** (Scheme 2).

The feasible route for the formation of the substituted nitrothiophene **4** is shown in Scheme 2. Attempts to isolate pure heterocycle **4** failed because of the low stability of this product and the presence of almost inseparable impurities. Nevertheless, *in situ* condensation with reactive dichloride precursor **1** gave the clathrochelate derivative **3** of this heterocycle, and this complex proved to be sufficiently stable to be isolated chromatographically. The second possible pathway to this complex (nucleophilic substitution with one of the two thiolate groups of mercaptomaleodinitrile at the first step) is also shown in Scheme 2.

A literature search for structural fragment **5** (Scheme 3) has revealed only two articles,[31,32] and they describe the different systems. This allows one to conclude that a previously unknown heterocyclic system has been obtained.

The synthesized complexes **2** and **3** were characterized by spectroscopic methods and X-ray crystallography. The asymmetric unit cell of crystal **2** contains two crystallographically independent clathrochelate molecules A and B with similar molecular structures (Figure 1) as well as the benzene solvate molecules. The coordination polyhedron of the encapsulated iron(II) ion possesses a distorted trigonal-prismatic (TP) geometry. The almost parallel triangular bases of the TP coordination polyhedron are formed by N1•N3•N5 and N2•N4•N6 nitrogen atoms, whereas its ribbed fragments are formed by N1•••N2, N3•••N4, and N5•••N6 chelate cycles. The average distortion angle φ in passing from a TP ($\varphi = 0°$) to a trigonal antiprism (TAP, $\varphi = 60°$) and the height h of the coordination polyhedron (the distance between the centers of the TP triangular bases) are equal to

(28) *SMART and SAINT, Release 5.0, Area Detector Control and Integration Software*; Bruker AXS: Madison, WI, 1998.
(29) Sheldrick, G. M. *SADABS: A Program for Exploiting the Redundancy of Area Detector X-Ray Data*; University of Göttingen: Göttingen, Germany, 1999.
(30) Sheldrick, G. M. *SHELXTL*, version 5.1; Bruker AXS: Madison, WI, 1997.
(31) Grol, C. J.; Rollema, H.; Dijkstra, D.; Westerink, B. H. C. *J. Med. Chem.* **1980**, *23*, 322.
(32) Grol, C. J.; Rollema, H. *J. Med. Chem.* **1975**, *18*, 857.

Table 2. Main Geometrical Parameters of Clathrochelate Molecules **2**, **3**, and **6**

	2			
param	type A	type B	**3**	**6**[22]
Fe−N (Å)	1.890(5)−1.920(5)	1.884(5)−1.904(5)	1.898(3)−1.916(3)	1.907(2)−1.919(2)
	av 1.901(6)	av 1.897(5)	av 1.905(3)	av 1.912
N−C (Å)	1.299(7)−1.330(7)	1.286(7)−1.331(7)	1.299(5)−1.314(5)	1.295(3)−1.310(4)
	av 1.312(7)	av 1.307(6)	av 1.307(5)	av 1.305(4)
N−O (Å)	1.356(6)−1.377(6)	1.358(6)−1.381(6)	1.376(4)–1.387(4)	1.362(3)−1.374(3)
	av 1.365(3)	av 1.368(6)	av 1.381(6)	av 1.369(3)
B1−O1 (Å)	1.498(8)	1.496(7)	1.494(6)	1.498(4)
B1−O3 (Å)	1.486(8)	1.489(7)	1.486(5)	1.481(4)
B1−O5 (Å)	1.471(8)	1.454(7)	1.487(5)	1.486(4)
B2−O2 (Å)	1.512(8)	1.509(7)	1.505(5)	1.501(4)
B2−O4 (Å)	1.450(8)	1.447(7)	1.470(5)	1.489(4)
B2−O6 (Å)	1.484(8)	1.487(7)	1.484(5)	1.483(4)
C1−C2 (Å)	1.418(8)	1.436(7)	1.454(5)	1.434(4)
C3−C4 (Å)	1.448(7)	1.457(7)	1.464(5)	
C5−C6 (Å)	1.469(7)	1.493(7)	1.462(5)	
C1−S1 (Å)	1.741(6)	1.760(7)		1.740(5)
C2−S2 (Å)	1.752(6)	1.748(6)		1.738(5)
S1−C9 (Å)	1.720(8)	1.723(7)		1.724(3)
S2−C7 (Å)	1.727(8)	1.736(7)		1.726(3)
C7−C9 (Å)	1.367(9)	1.365(9)		1.429(6)
N1−O1−B1 (deg)	110.6(5)	109.3(4)	109.4(3)	111.4(2)
N2−O2−B2 (deg)	110.8(5)	110.4(5)	108.7(3)	111.1(2)
N3−O3−B1 (deg)	110.9(5)	109.8(5)	112.5(3)	112.7(2)
N4−O4−B2 (deg)	112.6(5)	112.1(5)	112.6(3)	112.6(2)
N5−O5−B1 (deg)	114.1(4)	112.0(5)	112.5(3)	112.7(2)
N6−O6−B2 (deg)	111.8(5)	111.0(5)	111.1(3)	113.3(2)
Fe−N1−C1 (deg)	119.1(4)	117.8(4)	118.3(3)	117.7(2)
Fe−N2−C2 (deg)	117.3(4)	117.4(4)	118.7(3)	118.2(2)
Fe−N3−C3 (deg)	118.3(4)	119.3(4)	119.3(3)	119.3(2)
Fe−N4−C4 (deg)	119.5(4)	119.7(4)	119.8(3)	119.8(2)
Fe−N5−C5 (deg)	118.9(4)	120.6(4)	119.9(3)	119.5(2)
Fe−N6−C6 (deg)	119.7(4)	120.0(4)	119.5(3)	119.6(2)
Δ^a (deg)	29.7	30.0	2.4	15.6
φ^b (deg)	24.4	24.6	25.8	23.5
α^c (deg)	39.3	39.4	39.2	39.1
h^d (Å)	2.324	2.318	2.314	2.333

[a] Bend S···S (S···N) angle. [b] Distortion angle. [c] Bite angle (half the chelate angle). [d] Distance between the coordination polyhedron bases (the height of the distorted TP).

24.4° and 2.325 Å, respectively. The encapsulated iron(II) ion lies almost on the line that connects these centers (the corresponding angle is equal to 177.9°).

The dithiacyclohexane ribbed fragment of molecule **2** is nonplanar: the 1,4-dithiino-2,3-dicarbonitrile substituent has a boat conformation, and the dihedral angle Δ between its planar fragments with a bend along the S1···S2 line is approximately 30°.

The clathrochelate framework of the previously described[22] dithiine-containing clathrochelate **6** (Scheme 4) is identical to that of clathrochelate molecule **2**, but their functionalized ribbed fragments are different (the tricyclic 1,4-dithiino-2,3-quinoxaline fragment in the case of complex **6** instead of the monocyclic 1,4-dithiino-2,3-dicarbonitrile one in **2**). The TP iron(II) coordination polyhedron in molecule **6** is slightly less distorted than that in clathrochelate **2**. This might be accounted for by the influence of a bulkier tricyclic system that reduces the lability of the clathrochelate framework of **6**: the dithiine fragment in this molecule is drastically flattened (the bend along the S1···S2 line is half that in molecule **2**).

The B−O (B1−O1 and B2−O2) distances are higher and the N−O−B (N1−O1−B1 and N2−O2−B2) and Fe−N−C (Fe−N1−C1 and Fe−N2−C2) bond angles are smaller in the 1,4-dithiine-containing chelate fragment of the clathrochelate framework than the corresponding values for two diphenyl-substituted chelate cycles because of the effect of the high conjugation of the 1,4-dithiine moiety on the geometry of the functionalized dioximate ring.

Both crystals **2** and **6** contain benzene solvate molecules (**2**·2.5C_6H_6 and **6**·1.5C_6H_6). However, their crystal packings are different: in **6**·1.5C_6H_6, the crystal packing is determined by weak S2···F interactions, as well as by the diazine cycle of the quinoxaline system···solvate benzene molecule attractive interactions, whereas in **2**·2.5C_6H_6, the crystal packing is dictated by van der Waals interactions.

The asymmetric unit cell of crystal **3** contains one clathrochelate molecule, 2.5 solvate acetone molecules, and half a disordered solvate heptane molecule. The crystal packing of **3** is determined by van der Waals interactions.

The molecular structure of clathrochelate **3** (Figure 2) closely resembles that of complex **2**. The coordination polyhedron of the encapsulated iron(II) ion adopts a distorted TP geometry. TP triangular bases are formed by the N1·N3·N5 and N2·N4·N6 nitrogen atoms. The average distortion angle φ, bite angle α, and height h values are listed in Table 2.

As in the case of clathrochelate **2**, in molecule **3**, the B−O bond lengths are slightly longer, and the N−O−B and

Fe−N−C bond angles are slightly smaller in the NS-containing chelate fragment than those in phenyl-substituted fragments (Table 2). The NS-containing six-membered cycle is nearly planar (mean deviation is equal to 0.028 Å), and the C1−C2 bond is slightly shorter than the C3−C4 and C5−C6 bonds. An intramolecular weak hydrogen bond is formed by the NH group and the O8 atom of the adjacent nitro substituent.

The solution ^{1}H and $^{13}C\{^{1}H\}$ NMR spectra of complexes **2** and **3** confirmed the composition and symmetry of their molecules. The ^{1}H NMR spectrum of clathrochelate **2** contains only the broadened signal of the phenyl substituent protons at ∼7.3 ppm, whereas in the ^{1}H NMR spectrum of complex **3**, besides the line of this type, a new signal appears as the singlet line that is characteristic of the NH− proton in the expected ratio of line integral intensities (20:1). The ^{13}C NMR spectra of the clathrochelates obtained proved to be much more informative. The ^{13}C NMR spectrum of complex **2** confirmed both the composition and the presence of a symmetry plane passing through the middle of the chelate C−C bonds, the encapsulated iron(II) ion, and the middle of the C═C bond in the ribbed functionalized fragment. In particular, the singlet signal, assigned to azomethine carbon atoms in the PhC═N groups, was observed at ∼156 ppm. Such symmetry was not observed for molecule **3**, and its ^{13}C NMR spectrum contains two signals that were assigned to the azomethine carbon atoms of the nonequivalent PhC═N groups. This spectrum also contains the signals of the heterocyclic fragment carbon atoms.

The solution UV–vis spectrum of clathrochelate complex **3** also confirmed the absence of symmetry elements in this molecule. Six bands of high intensity (ϵ = ∼4 to 20 × 10^3 mol^{-1} L cm^{-1}) in the visible region were observed: they can be assigned to the Fed → Lπ^* charge transfer bands (CTBs). In contrast, in the UV–vis spectrum of complex **2** (the molecule of which has a symmetry plane), only two CTBs were observed in this region. The spectrum of clathrochelate complex **3** in the UV region contains the highly intensive bands that were assigned to the $\pi-\pi^*$ transitions in the conjugated α-dioximate fragments and some bands of close intensity assigned to the $\pi-\pi^*$ transitions in the ribbed annulated heterocyclic fragment. In the case of complex **2**, the number of bands that were assigned to the $\pi-\pi^*$ transitions in both the clathrochelate framework and the ribbed dithiadinitrile fragment is significantly less.

^{57}Fe Mössbauer parameters (isomeric shift [IS] and quadrupole splitting [QS]) of the clathrochelates **2** and **3** characterize them as low-spin iron(II) N_6 complexes with a TP−TAP geometry. QS values allow one to deduce the distortion angle φ values for these complexes with the use of a modern partial QS concept.[33] The distortion angle φ values for complexes **2** and **3** were calculated using a simple model:[33] $QS = PQS(12 - 18\cos^2\alpha/\cos^2(\varphi/2))$, where PQS is the partial quadrupole splitting with an approximate value of +0.5 mm s^{-1} for macrobicyclic tris-diiminates. The slightly increased QS values obtained for the synthesized compounds (see Experimental Procedures) as compared to those calculated from this equation (0.50 mm s^{-1} for **2** and 0.46 mm s^{-1} for **3**) can be accounted for by the fact that the molecules have no C_3 symmetry axis passing through the apical boron atoms and the central iron ion, and this induces an additional increase in the electric field gradient.

We plan to carry out the tetramerization of the dinitrile chlathrochelate **2** as well as the reaction of macrocyclization with phthalodinitrile, which leads to the formation of functionalized hybrid phthalocyanino-mono-, -di-, -tri-, and -tetra-clathrochelates. The intercalation into the DNA structure of intensive colored chlathrochelate **3** with an annulated highly conjugated π-system as a potential molecular probe will also be studied.

Acknowledgment. The authors gratefully acknowledge the support of the RFBR (Grants 05-03-33184, 06-03-32626, 06-03-90903, and 07-03-12183) and RAS (Program 7).

Supporting Information Available: Details of MALDI-TOF, IR, UV–vis, NMR, and Mössbauer data collections and listings of crystal and refinement data, bond distances, angles, and thermal parameters for **2** and **3**. This material is available free of charge via the Internet at http://pubs.acs.org.

IC701452G

(33) Voloshin, Y. Z.; Polshin, E. V.; Nazarenko, A. Y. *Hyperfine Interact.* **2002**, *141–142*, 309.